PCCP

Accepted Manuscript




ROYAL SOCIETY OF CHEMISTRY

www.rsc.org/pccp

# The Protonated and Sodiated Dimers of Proline by IRMPD Spectroscopy in the N-H and O-H Stretching Region and Computational Methods

Yasaman Jami Alahmadi, Ameneh Gholami, Travis D. Fridgen*

Department of Chemistry, Memorial University, St. John's, NL, Canada, A1B 3X7

*tfridgen@mun.ca

## Abstract

IRMPD spectroscopy and computational chemistry techniques have been used to determine that the proton- and sodium-bound dimers of proline exist as a mixture of a number of different structures. Simulated annealing computations were found to be helpful in determining unique structures for the protonated and sodiated dimers, augmenting chemical intuition. The experimental and computational results are most consistent with the proton-bound dimer existing N-protonated proline bound to zwitterionic proline. There was no spectroscopic evidence in the 3200-3800 $cm^{-1}$ region for a canonical structure which is predicted to have a weak N-H stretch at about 3440 $cm^{-1}$. A well resolved band at 1733 $cm^{-1}$ from a previous spectroscopic study (DOI: 10.1021/ja068715a) was reassigned from a high energy canonical isomer to the C=O stretch of a lower energy zwitterionic structure. This band is a free carboxylate C=O stretch where protonated proline is hydrogen bonded to the other carboxylate oxygen which is also involved in an intramolecular hydrogen bond. Fifteen structures for the sodium bound proline dimer were computed to be within 10 kJ $mol^{-1}$ in Gibbs energy and eight structures were within 5 kJ $mol^{-1}$. None of these structures can be ruled out based on the experimental IRMPD spectrum. They all have an N-H stretching band predicted in a position that agrees with the experimental spectrum. However, only structures where one of the proline monomers is in the canonical form and having a free O-H bond can produce the band at ~3600 $cm^{-1}$.

## 1. Introduction

Research on gas-phase ions and ion-molecule reactions provides us with information on intrinsic properties of ions. Mass spectrometric techniques are uniquely suited to determine reactivity and thermochemical properties for gas phase ions and can even be used to elicit structural characteristics. These techniques include blackbody infrared radiative dissociation (BIRD)[1,2,3,4] high pressure mass spectrometry (HPMS),[5,6,7,8,9] collision induced dissociation (CID),[10,11] high energy CID,[12,7,13,14] and the kinetic method.[15,16,17]

The three dimensional structures of biological macromolecules such as proteins are governed by non-covalent interactions such as hydrogen bonding and ionic hydrogen bonding. Typical ionic hydrogen bonds can be upwards of 130 kJ $mol^{-1}$, significantly stronger than the normal hydrogen bond.[18,19,20] The strength of these ionic hydrogen bonds and their ubiquitousness in biomacromolecules makes their fundamental study of utmost importance. Over the last decade, infrared multiphoton dissociation (IRMPD) spectroscopy[21,22,23,24] has been providing much more direct information into the subtleties of bonding, allowing for elucidation of the detailed structures of gaseous ions involving, for example, amino acids[21,22,25,26,27,28,29,30,31,32] and peptides.[22,33,34,35,36,37,38,39,40] IRMPD spectroscopy combined with electronic structure calculations is indeed a powerful combination of tools to help determine the structures of gas phase ions. Protonated amino acid dimers have been the topic of several recent IRMPD spectroscopic studies due to the existence of strong intermolecular ionic hydrogen bonding in these species as well as strong intramolecular hydrogen bonding interactions.[29,25,41,42,43,44] For example IRMPD spectroscopic studies on glycine, alanine, valine,[25] and serine[43] protonated dimers showed that the non-protonated amino acid in the dimer was canonical (ie. non-zwitterionic) but in the proline protonated dimer, neutral proline is predominantly zwitterionic.[42] Due to a band observed at 1733 $cm^{-1}$ which could not be ascribed

to the zwitterionic protonated dimer, Wu and McMahon[42] also concluded that an isomer where the neutral proline was in its canonical form was also present in the gas-phase mixture. These small proton-bound dimers can be models for larger systems where strong ionic hydrogen bonding exists, such as proteins. Metal ions also play a huge role in stabilizing biological polymers. Metal ion complexation can stabilize zwitterionic structures of amino acids depending on the size and valency of the metal atom and gas-phase basicity of the amino acids.[30,45,46]

Proline is one of the twenty common amino acids that comprise proteins and obviously plays an important role in human biology. Proline and its post-translationally modified analogue, hydroxyproline, are secondary amines and are among the main structural materials of fibrous proteins from which bones, tendons, ligaments, and skin are composed, owing to the rigidity of the cyclic structure.[47] Proline helps tissue repair following injuries such as burns, and after surgery.[48,49]

The present work is focused on the structural characterization of the protonated and sodiated dimers of proline using IRMPD spectroscopy in the N—H and O—H stretching region, 3200—4000 $cm^{-1}$. We also augment our experimental results with electronic structure calculations. Due to the existence of an immense number of possible structures for the gas phase ions under study, using only chemical intuition to come up with starting structures may not be a robust method to determine the global minimum. In order to fully explore the potential energy surface, different methods such as simulated annealing (SA) have been developed and used.[50,33,51]

## 2. Methods

**2.1. Experimental methods.** The protonated proline dimers, $[(Pro)_2H]^+$, were electrosprayed

from 100 micromolar aqueous solutions of proline to which a few drops of 100 micromolar aqueous formic acid were added. Similarly, the sodiated proline dimers, $[(Pro)_2Na]^+$, were electrosprayed from solutions to which a few drops of 100 micromolar NaCl were added. The laboratory for the study of energetics, reactions, and structures of gaseous ions at Memorial University houses an ApexQe Bruker FT-ICR mass spectrometer to which a tunable IR laser (OPO) has been mated. The coupling of these two instruments and their details have been published previously.[52,21,53] Briefly, the laser power is at a maximum of 60 mJ at about 3800 $cm^{-1}$ and decreases smoothly to about 10 mJ at 3100 $cm^{-1}$. Spectra presented in this paper have not been corrected for power fluctuations. Electrosprayed ions were stored in the hexapole storage cell for about 2 s before being transferred to the ICR cell where they were isolated by standard FT-ICR techniques. Ions were irradiated for 3 s at each wavenumber value between about 3820 and 3180 $cm^{-1}$ at 2 $cm^{-1}$ intervals. The IRMPD efficiency is the negative of the natural logarithm of the ratio of the precursor ion intensity over the sum of the precursor and fragment ion intensities. The IRMPD spectrum is a plot of the IRMPD efficiency vs wavenumber.

**2.2 Computational methods.** The AMBER9[54] suite of programs with the Generalized AMBER force field (GAFF)[55] was used to explore the conformational space of $[(Pro)_2H]^+$ and $[(Pro)_2Na]^+$. For the $[(Pro)_2Na]^+$ complexes Na was positioned in chemically relevant positions between the organic components and assigned an integer charge. Minimized energy conformations of the complexes were equilibrated for 10 ps at time steps of 0.5 fs at 300 K before undergoing 2000 cycles of simulated annealing (each 31 ps total, 0.5 in fs time step) starting with drastic heating from 300 K to 750 K over 3.00 ps and equilibrated for 1 ps. This was followed by cooling increments of 50K over 2 ps with 1 ps of equilibration at each temperature until 300 K. The lowest energy structure from each annealing cycle was used to

begin the subsequent round of simulated annealing. After each cycle the low energy conformation was cooled to 0 K over 5 ps, minimized, and the potential energy calculated.

Simulated annealing resulted in many different structures for $[(Pro)_2H]^+$ and $[(Pro)_2Na]^+$. For example, 8000 structures were obtained for $[(Pro)_2H]^+$ from four different simulated annealing runs, two for protonated proline complexed to zwitterionic proline, and two for protonated proline complexed with canonical proline. A potential energy vs simulated annealing cycle plot is shown in Fig.S1a of the supporting information for $[(Pro)_2H]^+$. Rearrangement of this data in order of energy along the abscissa reveals groups of structures with similar energies as can be seen in Fig. S1b. From the 8000 structures produced from the simulated annealing runs, about 120 unique structures were chosen for geometry optimization and frequency calculations using B3LYP/6-31+G(d,p). These optimized structures were then submitted to single point calculations using B3LYP in conjunction with the 6-311+G(3df,3pd) basis set. All ab initio and density functional calculations were done with the Gaussian 09[56] suite of programs. To compare the computed IR spectra with the experimental IRMPD spectra, the former were scaled by 0.964 along the wavenumber axis[57]. The relative enthalpies, $)_{rel}H$, and 298 K Gibbs energies, $)_{rel}G$, denoted as B3LYP/6-311+G(3df,3pd)//B3LYP/6-31+G(d,p) are the electronic energies from the single-point calculations combined with the thermal corrections to the enthalpy and Gibbs energy from the B3LYP/6-31+G(d,p) calculations and are reported relative to the lowest energy structure found. All relative energies are provided in kJ $mol^{-1}$ and were calculated using a temperature of 298 K. For comparison, geometry optimizations were done at the B3LYP/6-311+G(3df,3pd) and MP2/6-31+G(d,p) levels and basis sets and $)_{rel}H$ and 298 K $)_{rel}G$ were computed with these electronic energies with thermal corrections from the B3LYP/6-31+G(d,p) frequency calculations. MP2/6-311+G(3df,3pd) single point calculations were also

done on the MP2/6-31+G(d,p) optimized geometries. Finally, for comparison, dispersion corrected B3LYP (B3LYPD3) calculations using Grimme's D3 version with the original D3 damping function[58] were done with optimizations and frequency calculations using the 6-31+G(d,p) basis set and single point calculations using the 6-311+G(3df,3pd) basis. All the thermochemistries from these calculations are reported in Tables S1 and S2.

## 3. Results and Discussion

Upon resonant absorption of the infrared OPO laser, the only dissociation pathway observed was loss of proline for both $[(Pro)_2H]^+$ and $[(Pro)_2Na]^+$. The IRMPD spectra of $[(Pro)_2H]^+$ and $[(Pro)_2Na]^+$ are compared in Figure 1 in the 3200 − 3800 $cm^{-1}$ region. Both spectra contain a strong absorption at about 3600 $cm^{-1}$ corresponding to an O−H stretching vibration of a carboxylic acid group. Both also contain a feature associated with what is most likely an N-H stretch at 3400 $cm^{-1}$. The IRMPD spectrum of $[(Pro)_2H]^+$ also contains a broad absorption centered at about 3260 $cm^{-1}$ which most likely correspond to N-H stretches that are red shifted due to hydrogen bonding. These IRMPD spectra can be compared with infrared spectra computed for various isomers in order to help determine their structure. The structures and spectra of both $[(Pro)_2H]^+$ and $[(Pro)_2Na]^+$ are discussed in turn below.

**3.1. $[(Pro)_2H]^+$.** $[(Pro)_2H]^+$ consists of a protonated proline bound to a neutral proline. It is fundamentally important to know whether the neutral proline is zwitterionic (ZW) or canonical. In the literature when the amino acid is canonical and bound to an ion the structure has been coined "charge-solvated," (CS) and we adopt this term for the present paper.

A combination of simulated annealing and "chemical intuition" led to 42 unique structures for $[(Pro)_2H]^+$. Of these structures, 21 are within 16 kJ $mol^{-1}$ in Gibbs energy based on

MP2/6-311+G(3df,3pd)//B3LYP/6-31+G(d,p) calculations. There is good correlation in ordering and magnitude between the MP2 calculations and the B3LYP calculations as can be seen in Table S1. The ten lowest-energy structures are shown in Figure 2, and the remaining 11 below 16 kJ $mol^{-1}$ are shown in Fig. S2. Of the top 21 structures within 16 kJ $mol^{-1}$, one third are ZW, and 8 of the 10 lowest energy structures, in fact the six lowest, are ZW. The first two lowest energy structures differ only in ring puckering of the protonated proline (on the right side of each figure) and are separated by only 1.3 kJ $mol^{-1}$ in Gibbs energy according to the MP2/6-311+G(3df,3pd)//B3LYP/6-31+G(d,p) calculations. The conformations of the protonated proline in ZW1 and ZW2 are identical to the first and second lowest-energy structures determined by Marino et al[59] for bare protonated proline, exo and endo conformations, respectively, and with the carbonyl oxygen interacting with both the protonated amine and hydroxyl hydrogens. The zwitterionic prolines in both ZW1 and ZW2 are in endo conformations, similar to the lowest energy structure of neutral, non-zwitterionic proline.[59] ZW5 is similar to ZW1 except the ring puckering of the zwitterionic proline is exo, and is almost 5 kJ $mol^{-1}$ higher in Gibbs energy. The prolines in ZW3 have the same ring puckering as ZW1, but the two differ by what is effectively a rotation about the O—$H^+$-N. In all the zwitterionic structures, one of the carboxylate oxygens of the zwitterionic proline is involved in an intramolecular hydrogen bond to an amine hydrogen. In ZW1,2,3,5 and 6 the zwitterionic proline is bound to the protonated amine by the other carboxylate oxygen. In ZW4 and ZW8, however, the zwitterionic proline is bound through the same carboxylate oxygen that is also hydrogen bonded to the amine hydrogen, leaving one carboxylate oxygen free from any hydrogen bonding interactions. This is important as the infrared spectra for these two sets of ZW structures may be expected to be different in the C=O

stretching region, *vide infra*. ZW4 is only 3.7 kJ $mol^{-1}$ higher in energy than ZW1 while ZW8 which differs in ring puckering of the protonated proline, is 8.1 kJ $mol^{-1}$ relative to ZW1.

The lowest energy CS structure, CS7, is calculated to be 7.5 kJ $mol^{-1}$ higher in Gibbs energy than ZW1. The conformations of the prolines are identical in CS7 and ZW2, the only difference is neutral proline in the latter is zwitterionic.

In Figure 3, the computed spectra for the five lowest-energy ZW structures along with CS7 are compared to the experimental IRMPD spectrum. All the zwitterionic structures have virtually identical predicted spectra in the N-H/O-H stretching region, an O-H stretch at about 3600 $cm^{-1}$, and a free N-H stretch of the zwitterionic proline predicted at about 3390 $cm^{-1}$. A third vibration corresponds to the stretching of the N-H bond in protonated proline that is not bound to the neutral proline, but is involved in an intramolecular interaction with the carbonyl oxygen which is responsible for its red-shifting to between 3200 and 3300 $cm^{-1}$ from a normal amine N-H stretch. The fluctuation in the position of this band in different structures is due to that mode being sensitive to hydrogen bond strength. All of the ZW structures agree well with the experimental spectrum. The breadth of the experimental band at about 3260 $cm^{-1}$ is about 50 $cm^{-1}$ (fwhm) significantly broader than the 3600 $cm^{-1}$ band which is about 20 $cm^{-1}$ (fwhm). The range of predicted positions for the N-H stretch responsible for the feature 3260 $cm^{-1}$ are consistent with more than one structure being responsible for the observed infrared spectrum. This also consistent with so many (5) low-energy structures predicted to be within 5 kJ $mol^{-1}$ in Gibbs energy of the lowest energy structure. The other N-H stretch for the zwitterionic proline in the ZW structures is predicted to occur below 2850 $cm^{-1}$, strongly red-shifted due to a strong hydrogen bonding interaction with the carboxylate oxygen and outside the range of our laser.

The CS structures also have bands predicted at about 3600 $cm^{-1}$ and between 3200 and 3300 $cm^{-1}$, which correspond to the same vibrational modes as discussed above for the ZW structures. The difference is the free N-H stretch of the neutral proline. For the CS structures this band is predicted to be ~50 $cm^{-1}$ to the blue of that predicted for the zwitterionic structures. The predicted lower wavenumber N-H stretch for the ZW structure is due to a slight weakening of the free N-H bond due to protonation at N. While this band is weak, there is no sign of it in the experimental IRMPD spectrum and this is consistent with the predicted thermochemistry, being 7.5 kJ $mol^{-1}$ higher in energy corresponding to a population of only 4.9 % relative to ZW1. It is concluded, based on the agreement of the IR spectra of the ZW structures with the IRMPD spectrum and the computed thermochemistries, that $[(Pro)_2H]^+$ is zwitterionic.

Previous research has been conducted on the proton bound dimer of proline using IRMPD spectroscopy in the 1000 - 2000 $cm^{-1}$ region in conjunction with electronic structure calculations.[42] Their calculations showed that the four lowest energy structures of $[(Pro)_2H]^+$ were zwitterionic and the next seven structures are CS structures, more than 8 kJ $mol^{-1}$ in energy greater. The results presented here are perfectly consistent with Wu and McMahon in that the first CS structure is almost 8 kJ $mol^{-1}$ higher in energy than the lowest energy structure.[42] Their IRMPD spectrum also better matched the IR spectrum for a ZW structure consistent with our results in the 3200 – 3800 $cm^{-1}$ presented here. However, none of their ZW structures had a predicted band that could account for a nicely resolved band observed at 1733 $cm^{-1}$. Their lowest energy CS structure, identical to CS7 in Fig. 2 here, did have a predicted band matching the observed at 1733 $cm^{-1}$ due to the carbonyl of neutral proline, red shifted from the normal ~1800 $cm^{-1}$ position due to interaction with protonated proline. They concluded that the species responsible for their IRMPD spectrum were a combination of zwitterionic structures and the high

energy canonical structure. However we present another explanation for this 1733 $cm^{-1}$ band. ZW4 in Fig. 2 is 3.7 kJ $mol^{-1}$ lower in energy than CS7, and has a predicted C=O stretching vibration consistent with the 1733 $cm^{-1}$ band in the Wu and McMahon spectrum[42] (see Figure S3). The C=O stretch responsible for this band is the free carbonyl from zwitterionic proline which is blue shifted from the normal carboxylate C=O stretching position because it is not involved in a hydrogen bond; the other is involved in two hydrogen bonds.

The lowest energy structures for $[(Pro)_2H]^+$ were optimized using MP2/6-31+G(d,p) and the electronic energies were refined with MP2/6-311+G(3df,3pd) single point calculations. Dispersion corrected B3LYP calculations were also done for comparison. The thermochemistries computed for $[(Pro)_2H]^+$ structures are in Table S1 and are also included in Figure 2. It can be seen that the calculations using MP2/6-311+G(3df,3pd) on either the B3LYP/6-31+G(d,p) or MP2/6-31+G(d,p) geometries are consistent with a few minor differences. For example, structure ZW4 actually becomes the second lowest energy structure and higher in Gibbs energy than ZW1 by only 0.6 kJ $mol^{-1}$, corresponding to a ZW4 population 78 % that of ZW1. A simulated spectrum constructed of a weighted average of ZW1 and ZW4 in the 900 – 2000 $cm^{-1}$ region is provided in Fig. S3 and shows an excellent match to the experimental spectrum.

We conclude that the IRMPD spectra in both the 1000 – 2000 and 3200 – 3800 $cm^{-1}$ regions, as well as the computed thermochemistries are most consistent with a mixture of ZW structures and the lowest energy CS structure is probably a minor, unobserved component.

**3.2. $[(Pro)_2Na]^+$.** $[(Pro)_2Na]^+$ consists of a sodium cation bound to two proline dimers. Unlike the proton in $[(Pro)_2H]^+$, the sodium ion is more evenly shared between the two monomers. Simulated annealing calculations combined with chemical intuition resulted in 36 unique structures for $[(Pro)_2Na]^+$. The B3LYP/6-311+G(3df,3pd)//B3LYP/6-31+G(d,p) thermochemistries were used to rank the sodium bound dimer structures and it has been observed in the past that density functional theory provides better agreement with experimental thermochemistries for alkaline and alkaline earth metal containing complexes.[60]

The eight lowest energy structures are shown in Figure 4. The rest of the structures that were identified computationally are available in Fig. S4 and the thermochemistries are summarized in Table S2. Fifteen of these structures are within 10 kJ $mol^{-1}$ in Gibbs energy and in all of these at least one of the prolines is ZW. The lowest energy structures are a mixture of ZW-ZW, where both prolines are zwitterionic, and ZW-CS, where one of the prolines is canonical. The lowest energy CS-CS structure is about 12 kJ $mol^{-1}$ with respect to the lowest energy structure, ranked 18$^{th}$ of all the structures computed. This is consistent with previous research which shows that for the sodiated monomer, proline is zwitterionic,[45,61,62] so it would be expected that lower energy structures might have at least one of the prolines in its zwitterionic structure.

The O-H stretching band at 3600 $cm^{-1}$ in the IRMPD spectrum of the sodium bound dimer (Figure 5), clearly suggests that at least part of the population of observed ions contains a structure in which there is at least one canonical proline with a non-hydrogen bonded—or free—O-H bond. The ZW-ZW structures do not have a hydroxyl group, and the O-H stretch is red-shifted out of the range of the laser for ZW-CS structures (ie ZW-CS1 which has an identical predicted spectrum to ZW-CS3 in the N-H/O-H stretching region) where the hydroxyl group is

hydrogen bonded to the amine. However, structures such as ZW-CS4 and ZW-CS6 (which have identical predicted spectra in the N-H/O-H stretching region which are only 3.1 and 3.7 kJ $mol^{-1}$ higher in energy than the lowest energy structure, respectively, can account for the O-H stretching vibration with a free O-H moiety. In fact, ZW-CS4 is the lowest energy structure computed using dispersion corrected density functional theory (B3LYPD3, Table S2) with ZW-ZW2 and ZW-CS6 being 1.5 kJ $mol^{-1}$ higher in Gibbs energy. The relative intensities of the experimental N-H stretch and O-H stretch are also most consistent with the predicted spectrum for ZW-CS4 (and ZW-CS6). It is concluded that $[(Pro)_2H]^+$ is predominantly composed of a zwitterionic proline bound to $Na^+$ via the two carboxyl oxygens and the canonical proline is bound through the carbonyl O and the amine N with a free O-H bond that is observed to absorb at about 3600 $cm^{-1}$.

## 4. Conclusions

A combination of IRMPD spectroscopy and computational chemistry has been used to determine that the proton- and sodium-bound dimers of proline exist as a mixture of a number of different structures. Simulated annealing computations were also used to augment chemical intuition to determine unique structures of the dimeric complexes.

The proton-bound dimer structure exists as an N-protonated proline bound to zwitterionic proline. No spectroscopic evidence in the 3200-3800 $cm^{-1}$ region was observed for a canonical structure. A well resolved C=O band at 1733 $cm^{-1}$ from a previous spectroscopic study[42] was reassigned from a high energy canonical isomer to a lower energy zwitterionic structure.

Compuationally, there are many low energy sodium bound dimers of proline computed to be within 10 kJ $mol^{-1}$ in Gibbs energy and eight structures within 5 kJ $mol^{-1}$. None of the ZW-ZW structures can necessarily be ruled out based on the experimental spectrum. They all have an N-H stretching band predicted in the same position as that observed experimentally. However, only ZW-CS structures that have a free O-H bond can be responsible for the band at ~3600 $cm^{-1}$. The sodium-bound may exist as a number of different structures, but at least one of these must be a ZW-CS structure, such as ZW-CS4 with a free hydroxyl group. Diffusion corrected B3LYP calculations predict this ZW-CS4 structure to be the lowest-energy structure.

## 5. Acknowledgments

The authors acknowledge the financial contributions from the National Sciences and Engineering Research Council of Canada and the School of Graduate Studies at Memorial University that made this research possible. Westgrid and HPCVL is also acknowledged for the computational resources. Finally, the generous contribution of time from Justin Renault, a former PhD Student from Paul Mayer's group at the University of Ottawa, is greatly appreciated.

**Figure Captions**

Figure 1. Comparison of the IRMPD spectra from 3200 to 3800 $cm^{-1}$ for $[(Pro)_2H]^+$ (top) and $[(Pro)_2Na]^+$ (bottom).

Figure 2. Ten lowest energy structures for $[(Pro)_2H]^+$. MP2/6-311+G(3df,3pd)//B3LYP/6-31+G(d,p) and MP2/6-311+G(3dp,3pd)//MP2/6-31+G(d,p) (italicized) 298 K relative Gibbs energies, $)_{rel}G$, and enthalpies, $)_{rel}H$, (parentheses) are provided in kJ $mol^{-1}$.

Figure 3. Comparison of the experimental IRMPD spectrum for $[(Pro)_2H]^+$ with calculated IR spectra for different isomers of the dimer.

Figure 4. Eight lowest energy structures for $[(Pro)_2Na]^+$. B3LYP/6-311+G(3dp,3pd)//B3LYP/6-31+G(d,p), B3LYP/6-311+G(3df,3pd)//B3LYPD3/6-31+G(d,p) (italicized), 298 K $)_{rel}G$, and enthalpies, $)_{rel}H$, (parentheses) are provided in kJ $mol^{-1}$.

Figure 5. Comparison of the experimental IRMPD spectrum for $[(Pro)_2Na]^+$ with calculated IR spectra for different isomers of the dimer.

# References:

(1) Burt, M. B., Decker, S. G. A., and Fridgen, T. D. (2012) Water binding energies of [Pb(amino acid-H)H2O]+ complexes determined by blackbody infrared radiative dissociation. *Phys. Chem. Chem. Phys. 14*, 15118–15126.

(2) Gillis, E. A. L., Demireva, M., Sarwar, M. G., Chudzinski, M. G., Taylor, M. S., Williams, E. R., and Fridgen, T. D. (2013) Structure and energetics of gas phase halogen-bonding in mono-, bi-, and tri-dentate anion receptors as studied by BIRD. *Phys. Chem. Chem. Phys. 15*, 7638–7647.

(3) Dunbar, R. C. (2004) BIRD (blackbody infrared radiative dissociation): Evolution, principles, and applications. *Mass Spectrom. Rev. 23*, 127–158.

(4) Gillis, E. A. L., Demireva, M., Nanda, K., Beran, G., Williams, E. R., and Fridgen, T. D. (2012) Structures and energetics of electrosprayed uracilnCa2+ clusters (n = 14-4) in the gas phase. *Phys. Chem. Chem. Phys. 14*, 3304–3315.

(5) Wu, R., and McMahon, T. B. (2009) Structures, energetics, and dynamics of gas phase ions studied by FTICR and HPMS. *Mass Spectrom. Rev. 28*, 546–585.

(6) Wincel, H. (2007) Hydration of potassiated amino acids in the gas phase. *J. Am. Soc. Mass Spectrom. 18*, 2083–2089.

(7) Armentrout, P. B., and Heaton, A. (2012) Thermodynamics and Mechanisms of Protonated Diglycine Decomposition: A Guided Ion Beam Study. *J. Am. Soc. Mass Spectrom. 23*, 632–643.

(8) Wincel, H. (2007) Hydration Energies of Sodiated Amino Acids from Gas-Phase Equilibria Determinations. *J. Phys. Chem. A 111*, 5784–5791.

(9) Wincel, H. (2009) Microhydration of protonated nucleic acid bases and protonated nucleosides in the gas phase. *J. Am. Soc. Mass Spectrom. 20*, 1900–1905.

(10) Piatkivskyi, A., Osburn, S., Jaderberg, K., Grzetic, J., Steill, J. D., Oomens, J., Zhao, J., Lau, J. K.-C., Verkerk, U. H., Hopkinson, A. C., Siu, K. W. M., and Ryzhov, V. (2013) Structure and reactivity of the distonic and aromatic radical cations of tryptophan. *J. Am. Soc. Mass Spectrom. 24*, 513–23.

(11) Mayer, P. M., and Poon, C. (2009) The mechanisms of collisional activation of ions in mass spectrometry. *Mass Spectrom. Rev. 28*, 608–639.

(12) Yoo, J. S., Park, T., Bang, G., Lee, C., Rho, J.-R., and Kim, Y. H. (2013) High-energy collision-induced dissociation of [M+Na]+ ions desorbed by fast atom bombardment of ceramides isolated from the starfish Distolasterias nipon. *J. Mass Spectrom. 48*, 164–171.

(13) Carl, D. R., and Armentrout, P. B. (2012) Experimental Investigation of the Complete Inner Shell Hydration Energies of Ca2+: Threshold Collision-Induced Dissociation of Ca2+(H2O)x Complexes (x = 2–8). *J. Phys. Chem. A 116*, 3802–3815.

(14) Yang, Z., and Rodgers, M. T. (2012) Tautomerization in the formation and collision-induced dissociation of alkali metal cation-cytosine complexes. *Phys. Chem. Chem. Phys. 14*, 4517–4526.

(15) Kuntz, A., Boynton, A., David, G., Colyer, K., and Poutsma, J. (2002) The proton affinity of proline analogs using the kinetic method with full entropy analysis. *J. Am. Soc. Mass Spectrom. 13*, 72–81.

(16) Bouchoux, G. (2012) Gas phase basicities of polyfunctional molecules. Part 3: Amino acids. *Mass Spectrom. Rev. 31*, 391–435.

(17) Webb, I. K., Muetterties, C. E., Platner, C. B., and Poutsma, J. C. (2012) Gas-phase acidities of lysine homologues and proline analogs from the extended kinetic method. *Int. J. Mass Spectrom. 316–318*, 126–132.

(18) Fridgen, T. D., MacAleese, L., McMahon, T. B., Lemaire, J., and Maitre, P. (2006) Gas phase infrared multiple-photon dissociation spectra of methanol, ethanol and propanol proton-bound dimers, protonated propanol and the propanol/water proton-bound dimer. *Phys. Chem. Chem. Phys. 8*, 955–966.

(19) Burt, M. B., and Fridgen, T. D. (2007) Heterogeneous Proton-Bound Dimers with a High Dipole Moment Monomer: How Could We Experimentally Observe These Anomalous Ionic Hydrogen Bonds? *J. Phys. Chem. A 111*, 10738–10744.

(20) Meot-Ner (Mautner), M. (2012) Update 1 of: Strong Ionic Hydrogen Bonds. *Chem. Rev. 112*, PR22–PR103.

(21) Fridgen, T. D. (2009) Infrared consequence spectroscopy of gaseous protonated and metal ion cationized complexes. *Mass Spectrom. Rev. 28*, 586–607.

(22) Polfer, N. C., and Oomens, J. (2009) Vibrational spectroscopy of bare and solvated ionic complexes of biological relevance. *Mass Spectrom. Rev. 28*, 468–494.

(23) Eyler, J. R. (2009) Infrared multiple photon dissociation spectroscopy of ions in Penning traps. *Mass Spectrom. Rev. 28*, 448–467.

(24) Burt, M., and Fridgen, T. (2012) Structures and physical properties of gaseous metal cationized biological ions. *Eur. J. Mass Spectrom. 18*, 235–250.

(25) Rajabi, K., and Fridgen, T. D. (2007) Structures of Aliphatic Amino Acid Proton-Bound Dimers by Infrared Multiple Photon Dissociation Spectroscopy in the 700−2000 cm-1 Region. *J. Phys. Chem. A 112*, 23–30.

(26) Bush, M. F., Forbes, M. W., Jockusch, R. A., Oomens, J., Polfer, N. C., Saykally, R. J., and Williams, E. R. (2007) Infrared Spectroscopy of Cationized Lysine and ε-N-methyllysine in the Gas Phase: Effects of Alkali-Metal Ion Size and Proton Affinity on Zwitterion Stability. *J. Phys. Chem. A 111*, 7753–7760.

(27) Gholami, A., and Fridgen, T. D. (2013) Structures and Unimolecular Reactivity of Gas-Phase [Zn(Proline-H)]+ and [Zn(Proline-H)(H2O)]+. *J. Phys. Chem. B 117*, 8447–8456.

(28) Schmidt, J., and Kass, S. R. (2013) Zwitterion vs neutral structures of amino acids stabilized by a negatively charged site: infrared photodissociation and computations of proline-chloride anion. *J. Phys. Chem. A 117*, 4863–9.

(29) Atkins, C. G., Rajabi, K., Gillis, E. A. L., and Fridgen, T. D. (2008) Infrared Multiple Photon Dissociation Spectra of Proton- and Sodium Ion-Bound Glycine Dimers in the N−H and O−H Stretching Region. *J. Phys. Chem. A 112*, 10220–10225.

(30) Armentrout, P. B., Rodgers, M. T., Oomens, J., and Steill, J. D. (2008) Infrared Multiphoton Dissociation Spectroscopy of Cationized Serine: Effects of Alkali-Metal Cation Size on Gas-Phase Conformation. *J. Phys. Chem. A 112*, 2248–2257.

(31) Yang, B., Wu, R. R., Polfer, N. C., Berden, G., Oomens, J., and Rodgers, M. T. (2013) IRMPD action spectroscopy of alkali metal cation-cytosine complexes: effects of alkali metal cation size on gas phase conformation. *J. Am. Soc. Mass Spectrom. 24*, 1523–33.

(32) Gholami, A., and Fridgen, T. D. (2014) The unimolecular chemistry of [Zn(amino acid)2-H]+ in the gas phase: H2 elimination when the amino acid is a secondary amine. *Phys. Chem. Chem. Phys. 16*, 3134–3143.

(33) Semrouni, D., Balaj, O. P., Calvo, F., Correia, C. F., Clavaguéra, C., and Ohanessian, G. (2010) Structure of Sodiated Octa-Glycine: IRMPD Spectroscopy and Molecular Modeling. *J. Am. Soc. Mass Spectrom. 21*, 728–738.

(34) Bythell, B. J., Erlekam, U., Paizs, B., and Maître, P. (2009) Infrared Spectroscopy of Fragments from Doubly Protonated Tryptic Peptides. *ChemPhysChem 10*, 883–885.

(35) Prell, J. S., Flick, T. G., Oomens, J., Berden, G., and Williams, E. R. (2009) Coordination of Trivalent Metal Cations to Peptides: Results from IRMPD Spectroscopy and Theory. *J. Phys. Chem. A 114*, 854–860.

(36) Polfer, N. C., Oomens, J., and Dunbar, R. C. (2008) Alkali Metal Complexes of the Dipeptides PheAla and AlaPhe: IRMPD Spectroscopy. *ChemPhysChem 9*, 579–589.

(37) Zhao, J., Lau, J.-C., Grzetic, J., Verkerk, U., Oomens, J., Siu, K. W. M., and Hopkinson, A. (2013) Structures of a n * Ions Derived from Protonated Pentaglycine and Pentaalanine: Results from IRMPD Spectroscopy and DFT Calculations. *J. Am. Soc. Mass Spectrom. 24*, 1957–1968.

(38) Lanucara, F., Chiavarino, B., Scuderi, D., Maitre, P., Fornarini, S., and Crestoni, M. E. (2014) Kinetic control in the CID-induced elimination of H3PO4 from phosphorylated serine probed using IRMPD spectroscopy. *Chem. Commun. 50*, 3845–3848.

(39) Turecek, F., Moss, C. L., Pikalov, I., Pepin, R., Gulyuz, K., Polfer, N. C., Bush, M. F., Brown, J., Williams, J., and Richardson, K. (2013) Gas-phase structures of phosphopeptide ions: A difficult case. *Int. J. Mass Spectrom. 354–355*, 249–256.

(40) Dunbar, R. C., Berden, G., and Oomens, J. (2013) How does a small peptide choose how to bind a metal ion? IRMPD and computational survey of CS versus Iminol binding preferences. *Int. J. Mass Spectrom. 354–355*, 356–364.

(41) Wu, R., Marta, R., Martens, J., Eldridge, K., and McMahon, T. (2011) Experimental and Theoretical Investigation of the Proton-Bound Dimer of Lysine. *J. Am. Soc. Mass Spectrom. 22*, 1651–1659.

(42) Wu, R., and McMahon, T. B. (2007) Infrared Multiple Photon Dissociation Spectra of Proline and Glycine Proton-Bound Homodimers. Evidence for Zwitterionic Structure. *J. Am. Chem. Soc. 129*, 4864–4865.

(43) Kong, X., Tsai, I.-A., Sabu, S., Han, C.-C., Lee, Y. T., Chang, H.-C., Tu, S.-Y., Kung, A. H., and Wu, C.-C. (2006) Progressive Stabilization of Zwitterionic Structures in [H(Ser)2–8]+ Studied by Infrared Photodissociation Spectroscopy. *Angew. Chemie Int. Ed. 45*, 4130–4134.

(44) Oh, H.-B., Lin, C., Hwang, H. Y., Zhai, H., Breuker, K., Zabrouskov, V., Carpenter, B. K., and McLafferty, F. W. (2005) Infrared Photodissociation Spectroscopy of Electrosprayed Ions in a Fourier Transform Mass Spectrometer. *J. Am. Chem. Soc. 127*, 4076–4083.

(45) Kapota, C., Lemaire, J., Maître, P., and Ohanessian, G. (2004) Vibrational Signature of Charge Solvation vs Salt Bridge Isomers of Sodiated Amino Acids in the Gas Phase. *J. Am. Chem. Soc. 126*, 1836–1842.

(46) Bush, M. F., Oomens, J., Saykally, R. J., and Williams, E. R. (2008) Effects of Alkaline Earth Metal Ion Complexation on Amino Acid Zwitterion Stability: Results from Infrared Action Spectroscopy. *J. Am. Chem. Soc. 130*, 6463–6471.

(47) Lehninger, A., Nelson, D., and Cox, M. (2008) Lehninger Principles of Biochemistry. *Book*. W. H. Freeman.

(48) Stinnett, J. D., Alexander, J. W., Watanabe, C., Macmillan, B. G., Fischer, J. E., Morris, M. J., Trocki, O., Miskell, P., Edwards, L., and James, H. (1982) Plasma and Skeletal Muscle Amino Acids Following Severe Burn Injury in Patients and Experimental Animals. *Ann. Surg. 195*.

(49) Bergman, I., and Loxley, R. (1970) New spectrophotometric method for the determination of proline in tissue hydrolyzates. *Anal. Chem. 42*, 702–706.

(50) Comeau, A. N., Renaud, J. B., Mironov, G. G., Berezovski, M. V, and Mayer, P. M. (2012) Investigating the relationship between the gas-phase conformations and dissociation energetics of peptide–saccharide complexes. *Int. J. Mass Spectrom. 316–318*, 31–39.

(51) Zou, S., Oomens, J., and Polfer, N. C. (2012) Competition between diketopiperazine and oxazolone formation in water loss products from protonated ArgGly and GlyArg. *Int. J. Mass Spectrom. 316–318*, 12–17.

(52) Burt, M. B., Decker, S. G. A., Atkins, C. G., Rowsell, M., Peremans, A., and Fridgen, T. D. (2011) Structures of Bare and Hydrated [Pb(AminoAcid-H)]+ Complexes Using Infrared Multiple Photon Dissociation Spectroscopy. *J. Phys. Chem. B 115*, 11506–11518.

(53) Rajabi, K., Easterling, M., and Fridgen, T. (2009) Solvation of electrosprayed ions in the accumulation/collision hexapole of a hybrid Q-FTMS. *J. Am. Soc. Mass Spectrom. 20*, 411–418.

(54) Case, D., Darden, T. A., Cheatham, T. E., Simmerling, C., Wang, J., Duke, R., Luo, R., Crowley, M., Walker, R., Zhang, W., Merz, K. M., Wang, B., Hayik, S., Roitberg, A., Seabra, G., Kolossváry, I., Wong, K. F., Paesani, F., Vanicek, J., Wu, X., Brozell, S., Steinbrecher, T., Gohlke, H., Yang, L., Tan, C., Mongan, J., Hornak, V., Cui, G., Mathews, D. H., Seetin, M. G., Sagui, C., Babin, V., and Kollman, P. Amber 11 OR - University of California, San Francisco.

(55) Wang, J., Wolf, R. M., Caldwell, J. W., Kollman, P. A., and Case, D. A. (2004) Development and testing of a general amber force field. *J. Comput. Chem. 25*, 1157–1174.

(56) Frisch, M. J., Trucks, G. W., Schlegel, H. B., Scuseria, G. E., Robb, M. A., Cheeseman, J. R., Scalmani, G., Barone, V., Mennucci, B., Petersson, G. A., Nakatsuji, H., Caricato, M., Li, X., Hratchian, H. P., Izmaylov, A. F., Bloino, J., Zheng, G., Sonnenberg, J. L., Hada, M., Ehara, M., Toyota, K., Fukuda, R., Hasegawa, J., Ishida, M., Nakajima, T., Honda, Y., Kitao, O., Nakai, H., Vreven, T., Montgomery, J. A., Peralta, J. E., Ogliaro, F., Bearpark, M., Heyd, J. J., Brothers, E., Kudin, K. N., Staroverov, V. N., Kobayashi, R., Normand, J., Raghavachari, K., Rendell, A., Burant, J. C., Iyengar, S. S., Tomasi, J., Cossi, M., Rega, N., Millam, J. M., Klene, M., Knox, J. E., Cross, J. B., Bakken, V., Adamo, C., Jaramillo, J., Gomperts, R., Stratmann, R. E., Yazyev, O., Austin, A. J., Cammi, R., Pomelli, C., Ochterski, J. W., Martin, R. L., Morokuma, K., Zakrzewski, V. G., Voth, G. A., Salvador, P., Dannenberg, J. J., Dapprich, S., Daniels, A. D., Farkas, Foresman, J. B., Ortiz, J. V, Cioslowski, J., and Fox, D. J. (2009) Gaussian 09, Revision B.01. *Gaussian 09, Revis. B.01, Gaussian, Inc., Wallingford CT*. Wallingford CT.

(57) Moghaddam, M. B., and Fridgen, T. D. (2013) IRMPD Spectroscopic Study of Microsolvated [Na(GlyAla)]+ and [Ca(GlyAla–H)]+ and the Blue Shifting of the Hydrogen-Bonded Amide Stretch with Each Water Addition. *J. Phys. Chem. B 117*, 6157–6164.

(58) Grimme, S., Antony, J., Ehrlich, S., and Krieg, H. (2010) A consistent and accurate ab initio parametrization of density functional dispersion correction (DFT-D) for the 94 elements H-Pu. *J. Chem. Phys. 132*.

(59) Marino, T., Russo, N., Tocci, E., and Toscano, M. (2001) Density functional computations of proton affinity and gas-phase basicity of proline. *J. Mass Spectrom. 36*, 301–305.

(60) Zhu, W., Luo, X., Puah, C. M., Tan, X., Shen, J., Gu, J., Chen, K., and Jiang, H. (2004) The Multiplicity, Strength, and Nature of the Interaction of Nucleobases with Alkaline and Alkaline Earth Metal Cations: A Density Functional Theory Investigation. *J. Phys. Chem. A 108*, 4008–4018.

(61) Hoyau, S., Norrman, K., McMahon, T. B., and Ohanessian, G. (1999) A Quantitative Basis for a Scale of Na+ Affinities of Organic and Small Biological Molecules in the Gas Phase. *J. Am. Chem. Soc. 121*, 8864–8875.

(62) Marino, T., Russo, N., and Toscano, M. (2003) Interaction of Li+, Na+, and K+ with the Proline Amino Acid. Complexation Modes, Potential Energy Profiles, and Metal Ion Affinities. *J. Phys. Chem. B 107*, 2588–2594.

**Figure 1**.

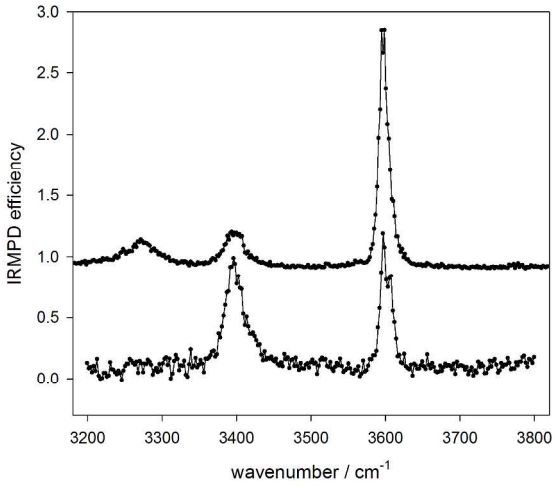


254x190mm (300 x 300 DPI)

**Figure 2.**

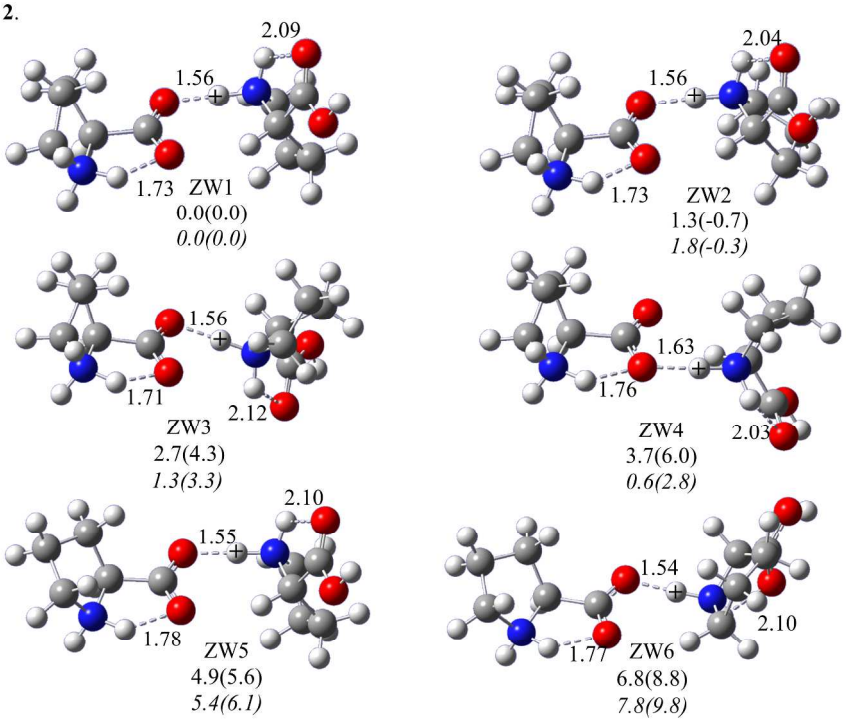


254x190mm (300 x 300 DPI)

**Figure 2 (cont'd).**

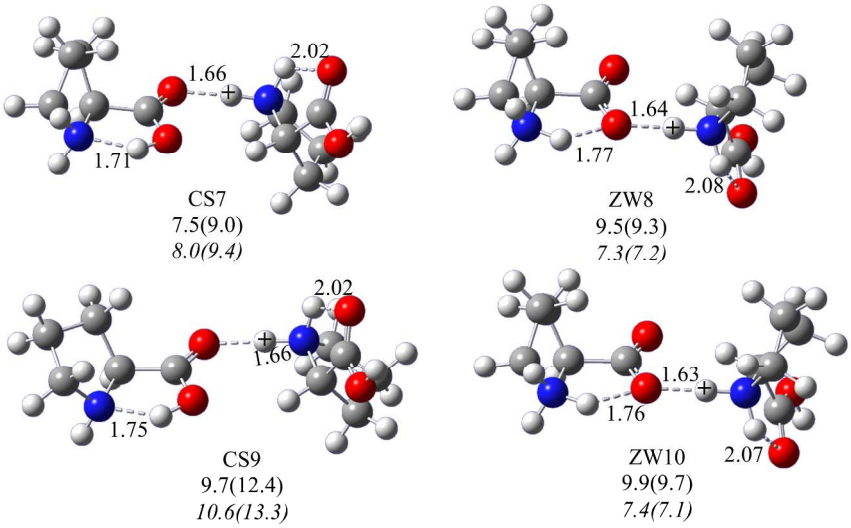


254x190mm (300 x 300 DPI)

**Figure 3**.

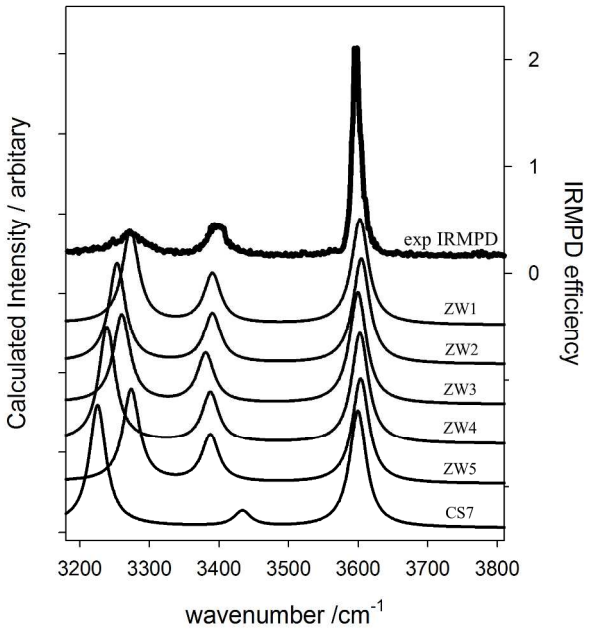


254x190mm (300 x 300 DPI)

**Figure 4.**

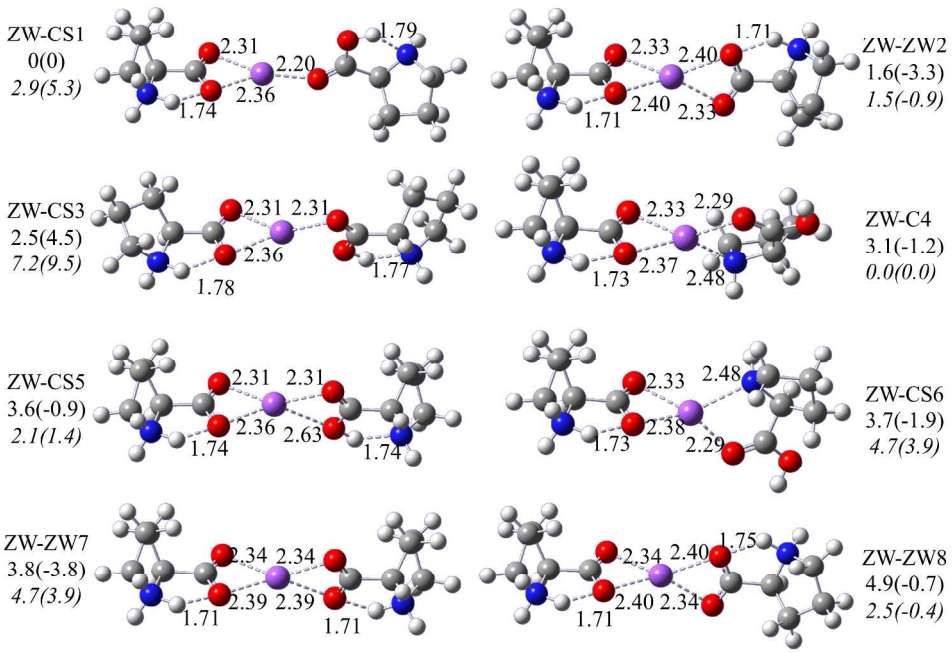


254x190mm (300 x 300 DPI)

**Figure 5.**

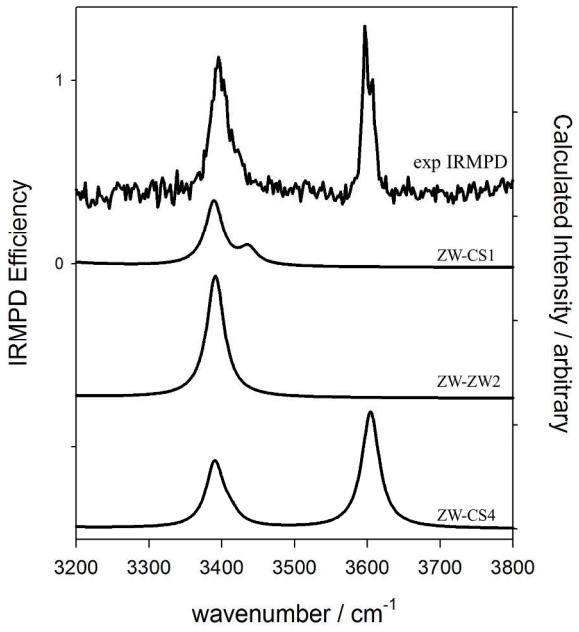


254x190mm (300 x 300 DPI)